Journal of Statistical Mechanics: Theory and Experiment
An IOP and SISSA journal

PAPER: Interdisciplinary statistical mechanics

Curling evolution of suspended threads replicates 2D self-avoiding walk phenomena and 1D crystallization process

H D Rahmayanti[1], R Munir[1], E Sustini[1] and M Abdullah[1,2]

[1] Department of Physics, Bandung Institute of Technology, Jl. Ganesa 10, Bandung 40132, Indonesia
E-mail: mikrajuddin@gmail.com

Received 27 March 2018
Accepted for publication 23 November 2018
Published 4 January 2019

Online at stacks.iop.org/JSTAT/2019/013401
https://doi.org/10.1088/1742-5468/aaf322

Abstract. The conformation evolution of threads that fall freely after being released from varying altitudes was investigated and compared to behaviors generated by other well-known fundamental physical processes. It was observed that the thread conformation replicated the conformation of long polymer chains, motivating the authors to apply a 2D self-avoiding walk (SAW) model to explain their stable conformation. Strong evidence was identified that the thread conformation strongly resembles 2D SAW behavior and has scaling power comparable to that of a 2D SAW. Also, by fitting how thread end-to-end distance evolves with time, an equation was obtained that is exactly identical to the modified Avrami equation, which is usually used for explaining phase transformation processes in 1D space ($D = 1$). The exponential power of $n = D + 1 = 2$ was simply obtained in our fitting. In conclusion, it can strongly be stated that the evolution of thread conformation over time replicates the crystallization process in 1D space and an SAW in a 2D space, showing that these microscopic processes can be replicated at macroscopic scale.

Keywords: classical phase transitions, random graphs, networks

[2] Author to whom any correspondence should be addressed.

1742-5468/19/013401+16$33.00

Contents

1. Introduction

If we release a horizontally stretched thread to fall freely, the thread shape becomes curly. Specifically, the end-to-end distance becomes shorter and the shape resembles that of long polymer chains observed under an electron microscope. Interestingly, the shape shrinks as time lapses and is likely to reach a stable size, where further time lapse does not change the size while the curly orientation may still change. This means that the thread will evolve to attain final conformation.

The shapes of polymer chains have been explained using the SAW model [1, 2]. In many situations the model successfully explains the chain conformation, including accurate estimation of end-to-end distance and radius of gyration as a function of chain length [3, 4]. Since the shape of the thread resembles that of a polymer chain, it is challenging to explore potential application of the SAW model to explain the conformation of threads after reaching stable size (after being left to fall from high altitude). This exploration is interesting since it is a simple macroscopic demonstration of the SAW phenomenon that can be observed by the naked eye.

Letting threads to fall freely from a high altitude may seem like an unimportant phenomenon, since many people experience it and seemingly nothing interesting can be extracted from its observation. However, it will be shown here that this phenomenon may attract a lot of attention since it exhibits several interesting physical phenomena. Indeed, there are many common phenomena around us that could be interesting topics of research that have not been considered as such by many people [5–12]. Explorations of 'common phenomena' in order to show richness of physical phenomena have been reported, such as walking with coffee [9], capillary force repelling the coffee-ring effect [13], fingering structures inside the coffee ring [14], shapes of a suspended curly hair [5], bending of sparklers [10], and wringing of wet cloth [7].

The phenomenon of the free fall of a thread can be investigated further by asking what the influence is of changing the thread material and wetting the thread (since different wetting liquids lead to different elastic properties of the thread) on the final

J. Stat. Mech. (2019) 013401

conformation. Does the behavior approximate that of SAW phenomena at microscopic scale?

The objective of this work was to explore the shape of free falling threads and to find its correlation with SAW phenomena. This work also aimed to prove the occurrence of SAW phenomena at macroscopic scale. Simple experiments were performed and mathematical formulae were derived to describe the experimental results. However, it must be noted that the effect of gravity was not taken into account. The free-falling process was solely employed for producing free conformation conditions (air friction only) starting from the thread in a straight state until it reaches stable conformation. This is an easier way to generate such conditions compared to suspending threads with some kind of upward force for example.

2. Experiment

In the experiment, three types of threads were used: wool, mélange and multifilament. The length of the threads was varied between 0.5 m, 0.75 mn, 1 m, 1.25 m, 2 m, and 2.5 m. We applied three mechanical conditions to the threads: dry, wetted with water, and wetted with alcohol. Water and alcohol have different surface tension (around 0.023 N m^{-1} for ethyl alcohol [15] and around 0.073 N m^{-1} for water [15, 16]). The difference in surface tension was expected to affect the mechanical properties of the thread and influence the final end-to-end distance. The threads were released from an altitude of up to 22.5 m and positioned horizontally to ensure stable conformation was developed. The time it took for the threads to touch the ground was also recorded. After the threads touched the ground, the end-to-end distance was measured. Repetitions between 6 and 10 times were conducted for each experimental condition.

After being released from different altitudes, pictures were taken of the threads while falling and after touching the ground to show their conformation. The threads were immersed in a luminescent liquid beforehand and the pictures were taken in the dark under specific light illumination to show the conformation of the threads more clearly. The reason for using luminescent liquid was that the threads were very thin and their colors were not strongly different from the background (tiles).

3. Experimental results

Figure 1 shows images of the different threads used: (a) wool, (b) mélange and (c) multifilament released at different altitudes: (i) 0.5 m, (ii) 1.5 m and (iii) 2.5 m; all had the same length (0.5 m). As mentioned above, the pictures were taken in the dark using a specific light source so the threads glowed up after they touched the ground. It can clearly be seen that all threads formed conformations nearly identical to that of polymer chains, especially the threads that were released from higher altitudes. Generally, curling conformation increased when the altitude was increased. This means that the initial state, when the thread was straight, was very unstable. Under free

J. Stat. Mech. (2019) 013401

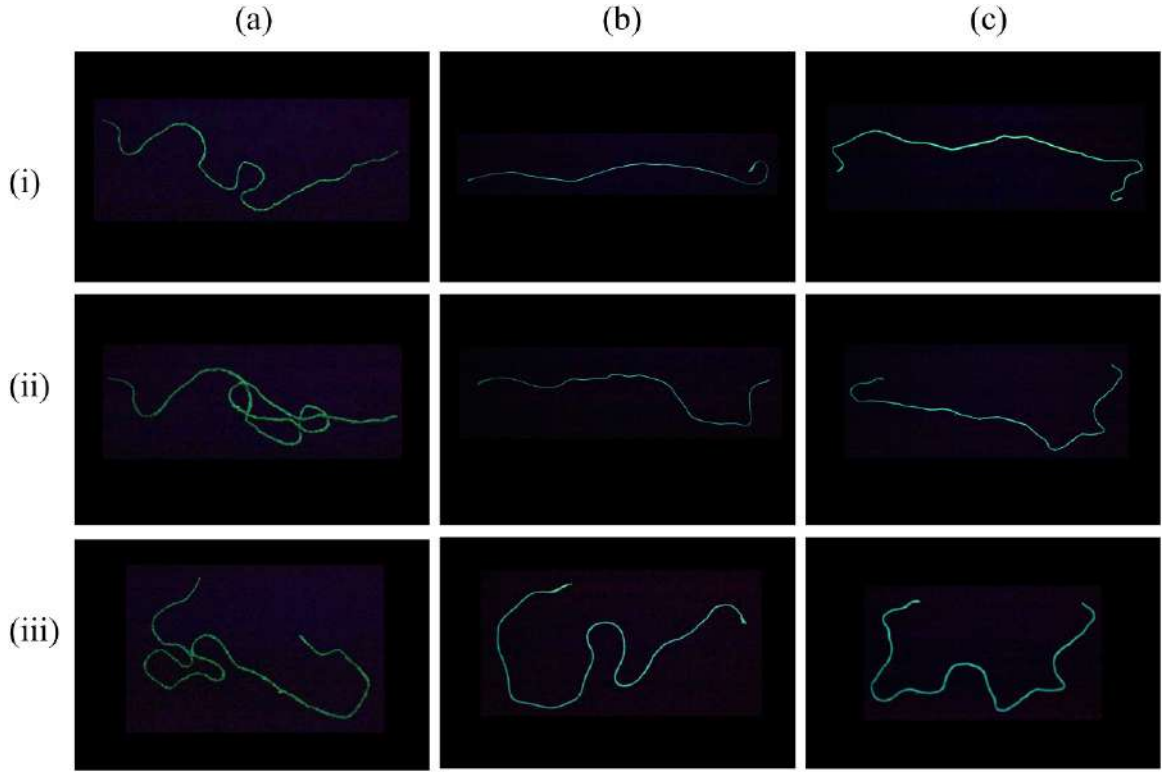

Figure 1. Topologies of the threads after touching the ground. The threads glowed under specific light illumination. Three different threads were used: (a) wool, (b) mélange, and (c) multifilament. They had the same length (0.5 m) and were released from different altitudes: (i) 0.5 m, (ii) 1.5 m, and (iii) 2.5 m.

release (assuming the interaction of the thread with molecules in the air was negligible), the thread evolved into stable conformation. It can also be seen that the conformation of the threads was closely related to an SAW.

The final conformation was also inspected under variation of the thread length. Figure 2 (left) shows the final topologies of the multifilament threads released at an altitude of 1.0 m. Three different lengths were used: 0.5 m, 0.75 m, and 1.0 m. Longer threads correspond to longer SAWs (time proportional to thread length).

The effect of wetting liquid on the conformation was also inspected. The topologies of dry wool, wool wetted with alcohol, and wool wetted with water were compared. Three threads of the same length (0.5 m) were released from the same altitude of 0.5 m. As shown in figure 2 (middle), dry wool tended to form a straight conformation, while wool wetted with water tended to form a more curly conformation. This means that dry wool is much harder to bend and the wool wetted with water is the most easily bent.

Microscopic images of the samples were also recorded. Images of wool threads are shown in figure 2 (right): (a) camera picture of dry wool, (b) microscopic image of wool wetted with alcohol, and (c) microscopic image of wool wetted with water. It is likely that the wool absorbs more water than alcohol, causing the wool wetted with water to become much more weak than the dry wool or the wool wetted with alcohol.

J. Stat. Mech. (2019) 013401

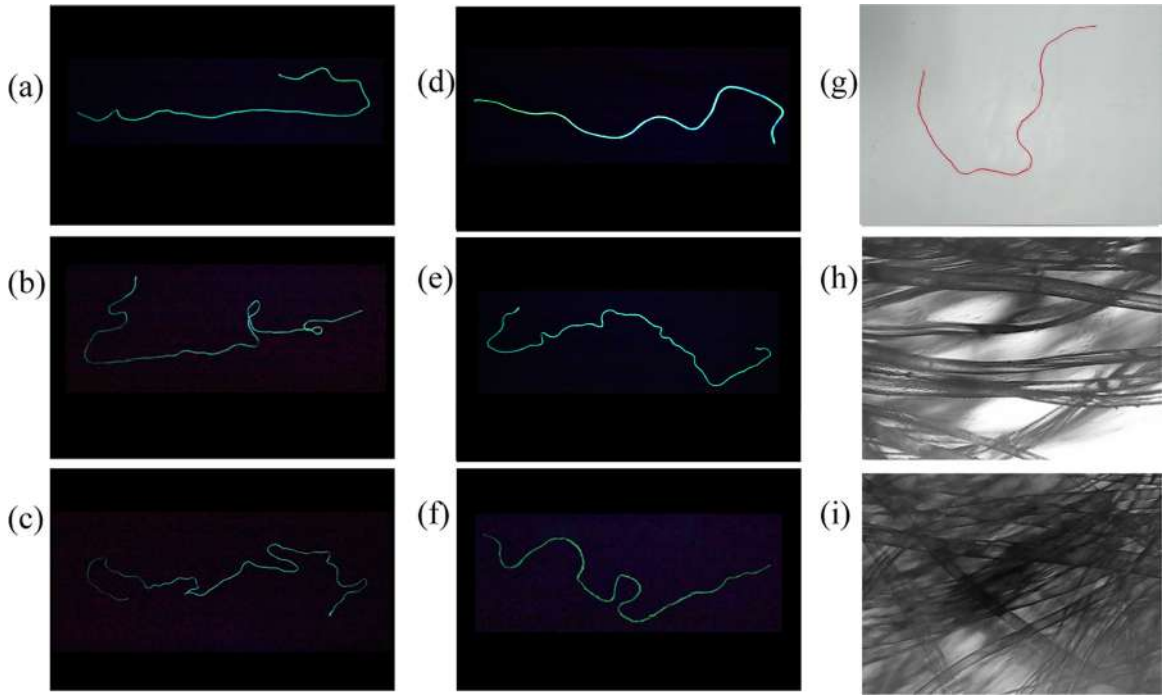

Figure 2. (Left) Images of multifilament threads of different lengths: (a) 0.5 m, (b) 0.75 m, and (c) 1.0 m, released from the same altitude of 1.0 m. (Middle) Images of wool of 0.5 m length with different wetting liquids released from the same altitude of 0.5 m: (d) dry wool, (e) wool wetted with alcohol, (f) wool wetted with water. (Right) Image of (g) dry wool recorded using a digital camera, and images of (h) wool wetted with alcohol, and (i) wool wetted with water, both recorded using an optical microscope.

It is also interesting to investigate whether the conformation obeys a 2D or a 3D topology. For clarification, horizontally oriented pictures were taken of the falling threads. Figure 3 shows side images of the falling threads. The threads were also recorded using a video camera. The images in figure 3 are frames depicting a thread of 0.75 m length at different times, which was dropped from an altitude of 4 m from the ground. The appearance of the threads had insufficient contrast so we used rectangles to indicate the curl boundaries. It was observed that the thread conformation was not only occurred within a horizontal plane (2D conformation) but slightly expanded in a vertical direction, which means that the conformation is 3D. However, the vertical dimension was much smaller than the horizontal dimension so that in this work it was approximated as 2D conformation.

The threads' end-to-end distances were then measured under different conditions: different types of thread, different altitudes for release, and different wetting liquids to inspect whether the curly conformation of the threads had a correlation with the SAW model. A SAW model was used instead of simple random walk since the threads behave like polymer chains, so that it is impossible for random walk to visit the same site more than once. The most important parameter is the power factor, relating the walk time to the end-to-end distance. If the threads are divided into a large number of segments, the segment length corresponds to distance traveled at one time step while the thread length corresponds to the total time of the SAW. The same as in the simple

J. Stat. Mech. (2019) 013401

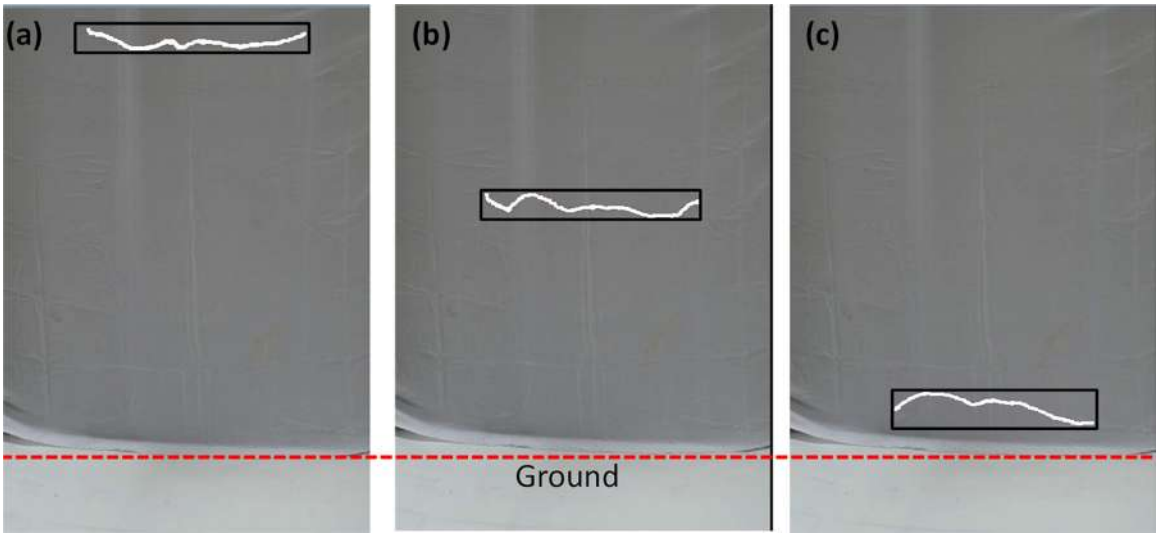

Figure 3. Images of falling threads recorded from the side. The view is oriented horizontally. Images (a)–(c) represent the threads at different altitudes ((a)–(c) means they are approaching the ground). The appearance of the threads had insufficient contrast so we used rectangles to indicate the curl boundaries. The images depict a thread of 0.75 m length after being released from an altitude of 4 m.

random walk model, in the SAW model the end-to-end distance satisfies $\sqrt{\langle r^2 \rangle} \propto t^{\kappa}$ with t is time and κ is the scaling factor depending on the dimension (=1, 0.75, and 0.588 for one, two, and three dimensions, respectively) [17]. In a simple random walk model we have $\kappa = 0.5$, which is the same as κ for an SAW in 4D. In the present work, what needed to be inspected was if the same relation will also been obtained for a 2D SAW, i.e. $\sqrt{\langle r^2 \rangle} \propto L^{\kappa}$ with L is the thread length and κ is the scaling parameter. As explained above, the conformation of the released threads approximated a 2D conformation, although slight stretches in the vertical dimension were observed (which were ignored in this work). The tendency to form a 2D conformation is due to gravitation, which attracts the thread elements simultaneously (under the assumption that air friction is identical for all segments). Slight spreading into a 3D conformation is caused by different air frictions experienced by different segments or the internal arrangement of the thread to maintain energy conservation.

The threads were dropped starting from a straight horizontal position. The shape evolved to curly and the end-to-end distance decreased progressively. The question is how much time is required for the thread to reach stable conformation, i.e. when the end-to-end distance is saturated. For this purpose, the threads were dropped from a building from an altitude of up to 22.5 m from the ground. Figure 4 shows the data of the end-to-end distance of the threads for different materials in three length variations and the same threads wetted with different liquids. From all figures it is clear that a stable end-to-end distance was obtained after the threads had fallen for about 5 m. The end-to-end distance remained relatively unchanged after dropping from an attitude 5 m to 22.5 m. It is also clear that the end-to-end distance decreased as the thread length decreased. Therefore, the relation $\sqrt{\langle r^2 \rangle} \propto L^{\kappa}$ seems to be acceptable. What needed to

J. Stat. Mech. (2019) 013401

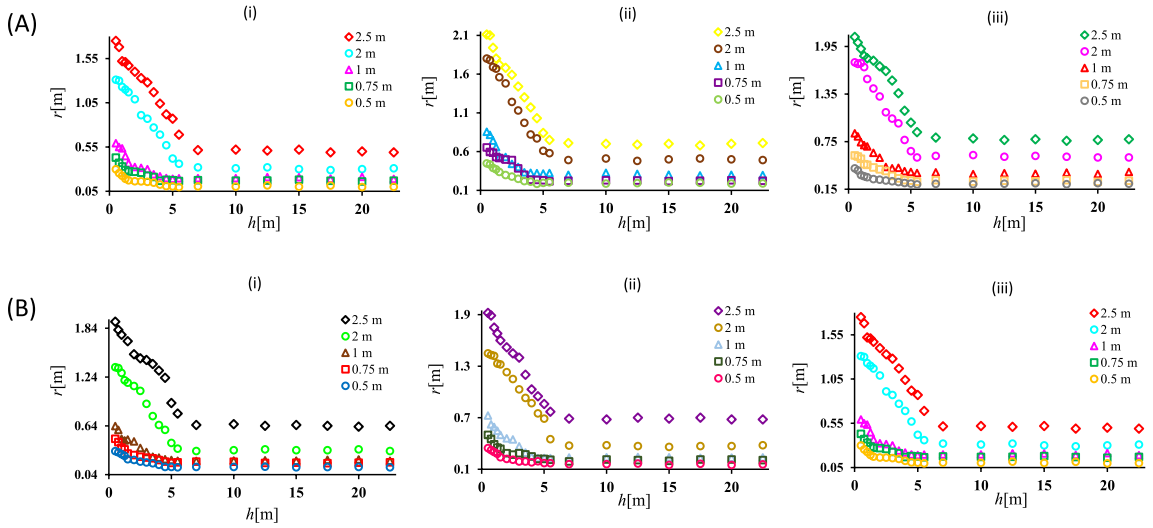

Figure 4. Effect of altitude on the end-to-end distance of the threads. Upper figures (A): (i) wool thread, (ii) mélange thread, and (iii) multifilament thread. The length of all three threads was varied between 0.5 m, 0.75 m, 1.0 m, 2 m, and 2.5 m. Bottom figures (B): (i) dry wool, (ii) wool wetted with alcohol, and (iii) wool wetted with water. The symbols indicate measured data and the curves display the fitting results.

be further explored was the value of parameter κ. Is this parameter consistent with the corresponding parameter for an SAW process?

At the same time, the relationship between falling time and falling distance was also measured. For example, figure 5 shows a plot of falling distance against falling time for: (a) dry wool and (b) wool wetted with alcohol. Both materials showed a linear relationship between falling time and falling distance, indicating that both quickly reached terminal velocity. The terminal velocities were obtained by fitting the data with a linear function, where the slope of the curve represents the terminal velocity. The terminal velocities for all dry wools were nearly the same (1.06–1.14 m s^{-1} with $0.992 < R^2 < 0.999$). Similarly, the terminal velocities for all wools wetted with alcohol were also nearly the same (in the range between 2.68 and 2.96 m s^{-1} with $0.994 < R^2 < 998$). The terminal velocity of wool wetted with water was clearly higher than that of dry wool.

Figure 6 shows a plot of $\ln r$ (r is the average end-to-end distance) with respect to $\ln L$ for: (a) wool wetted with water, (b) mélange thread wetted with water, and (c) multifilament thread wetted with water. The symbols indicate the measurement results. The data clearly show a linear relationship between $\ln r$ and $\ln L$. Based on the fitting results, the gradients obtained for the lines were: $\kappa = 0.895$, 0.798, and 0.794 for wool thread wetted with water, mélange thread wetted with water, and multifilament thread wetted with water, respectively. The three collected data sets satisfied the following fitting equations: $\ln r = 0.895 \ln L - 1.593$ ($R^2 = 0.958$), $\ln r = 0.798 \ln L - 1.170$ ($R^2 = 0.974$), and $\ln r = 0.794 \ln L - 1.050$ ($R^2 = 0.976$), for wool thread wetted with water, mélange thread wetted with water, and multifilament thread wetted with water, respectively. Based on the scaling factors obtained from fitting it could be deduced that the scaling factors for the three materials were between the scaling factors of 1D SAW

https://doi.org/10.1088/1742-5468/aaf322

J. Stat. Mech. (2019) 013401

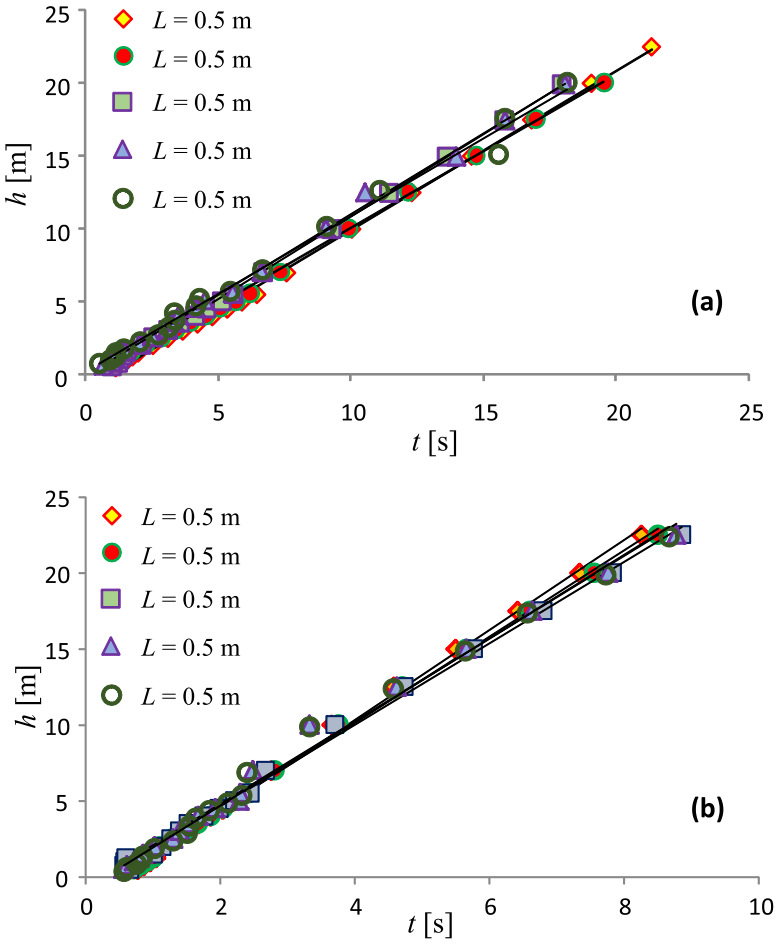

Figure 5. Plot of falling distance (h) with respect to falling time (t) of: (A) dry wool and (B) wool wetted with alcohol. Symbols indicate measured data and the curves display the linear fitting results.

(1.0) and 2D SAW (0.75). It is also interesting to observe that the resulted scaling factors for the three materials were almost identical. They were different by 0.1 only.

Figure 7 shows the same data for wool wetted with different liquids: (a) dry wool, (b) wool wetted with alcohol, and (c) wool wetted with water. Here also, the data clearly show a linear relationship between $\ln r$ and $\ln L$. The three collected data sets satisfy the following fitting equations: $\ln r = 0.834 \ln L - 1.338$, $\ln r = 0.879 \ln L - 1.447$, and $\ln r = 0.895 \ln L - 1.595$, for dry wool, wool wetted with alcohol, and wool wetted with water, respectively. The estimated scaling factors were also between the scaling factors of 1D SAW (1.0) and 2D SAW (0.75). It can thus be concluded from figures 6 and 7 that, in spite of slight conformation stretching in the vertical direction, the 3D behavior is negligible. Also, based on the values of the scaling factor, the 2D SAW is more dominant than the 1D SAW. Therefore, in the rest of this paper the thread conformation is considered as being controlled by a 2D SAW.

J. Stat. Mech. (2019) 013401

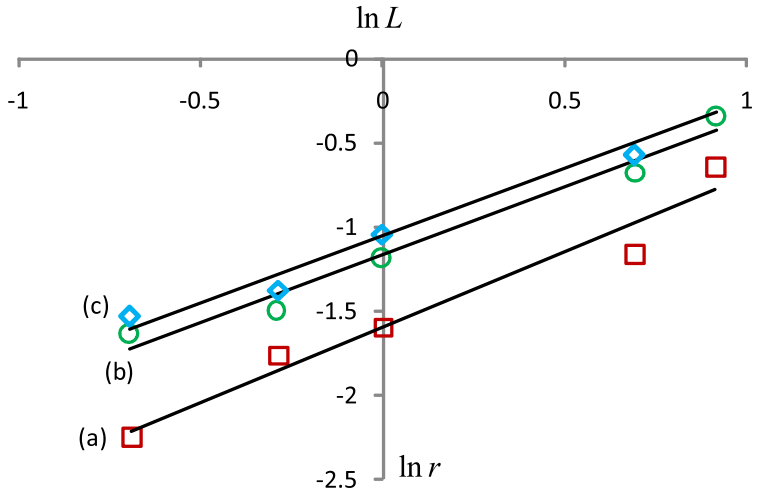

Figure 6. Effect of thread length on end-to-end distance assuming that a stable distance has been reached: (a) wool thread wetted with water, (b) mélange thread wetted with water, and (c) multifilament thread wetted with water. The fitting equations $\ln r = 0.895 \ln L - 1.593$, $\ln r = 0.798 \ln L - 1.170$ and $\ln r = 0.794 \ln L - 1.050$ were obtained for wool thread wetted with water, mélange thread wetted with water, and multifilament thread wetted with water, respectively.

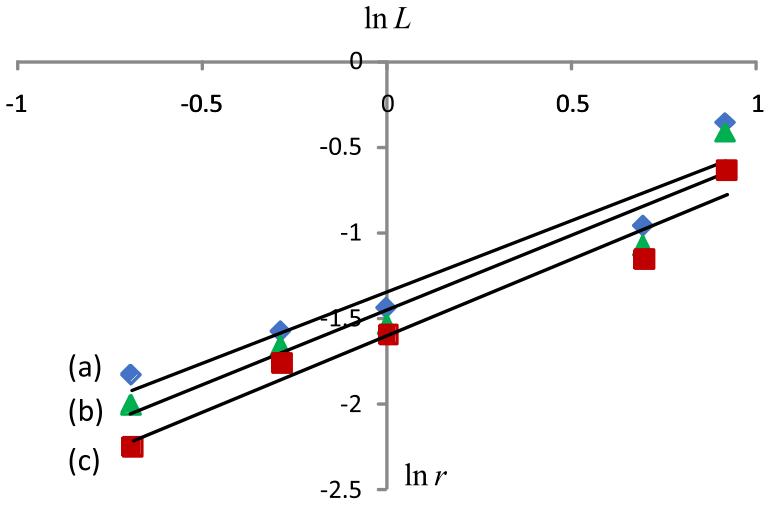

Figure 7. Effect of thread length on end-to-end distance for (a) dry wool, (b) wool wetted with alcohol, and (c) wool wetted with water. The following corresponding fitting equations were obtained: (a) $\ln r = 0.834 \ln L - 1.338$, $R^2 = 0.923$; (b) $\ln r = 0.879 \ln L - 1.447$, $R^2 = 0.920$; and (c) $\ln r = 0.895 \ln L - 1.595$, $R^2 = 0.958$.

4. Modelling

The random walk model is commonly used for explaining the random motion of particles, such as the Brownian motion of particles in a suspension. In this model, the particle is allowed to visit the same site at different times. However, in case of polymer conformation, if a certain site has been occupied (visited) by a monomer, such a

J. Stat. Mech. (2019) 013401

monomer stays at that site to reject the visit of other monomers. This is a key assumption of the SAW model, which is why it is best to use the SAW model to describe polymer conformation. As mentioned above, thread conformation likely duplicates polymer conformation and therefore we used a SAW model to describe the thread conformation. The repulsive energy for a walk of N steps stretching out over distance r in a space with fractal dimension $\bar{d}$ can be approximated as [18]:

$$U \approx N^2 r^{-\bar{d}}. \tag{1}$$

This expression also represents the repulsive energy experienced by a polymer chain in a dilute solution [19] and we may consider air as a very dilute solution. The entropy was estimated under the assumption of a Gaussian distribution of the distance r travelled in a random walk after N steps. The probability distribution of end-to-end distance in a 2D vector space with a limit of $N \to \infty$ is given by the Gaussian distribution function $P(\vec{r}) = \Psi(N)\exp(-r^2/r_0^2)$, with $\Psi(N)$ is a function of N and r_0 increases as a power of N [17, 19], $r_0 \propto N^{1/d_w}$, with d_w is the diffusion dimension defined by $r^{d_w} \approx t$ for very large t (time elapsed for random walk). Both $\bar{d}$ and d_w are related by equation $\bar{d} + \zeta = d_w$, with ζ is the resistivity exponent defined by $\Omega(r) \approx r^{\zeta}$ for the resistivity Ω between two points at a distance r.

The entropy difference between a thread with end-to-end distance $\vec{r}$ and one with an end-to-end vector of zero is $S \propto \ln P(\vec{r})/P(0)$, or:

$$S \approx -r^2 N^{-2/d_w}. \tag{2}$$

Based on equations (1) and (2), the Helmholtz free energy $F = U - TS$ is estimated as:

$$F \approx N^2 r^{-\bar{d}} + T r^2 N^{-2/d_w} \tag{3}$$

with T is temperature. The standard thermodynamic expression for free energy is used, including the introduction of an absolute temperature in the entropy part, even though the system is macroscopic. Indeed, a similar treatment for macroscopic systems has been considered using a microscopic equation. For example, Rosato *et al* have considered the Brazil nuts effect of a mixture of small and large intruders in a shaking container by applying the Maxwell–Boltzmann distribution function for the particles even though the particle masses were very large [20]. Several authors have considered the granular system to behave like a gas and equations that are applied to gas were applied to a granular system (macroscopic size) [21, 22]. The equilibrium state is obtained by minimizing F to produce $-\bar{d}N^2 r^{-\bar{d}} + 2TrN^{-2/d_w} \approx 0$, resulting in:

$$r \approx \left(\frac{\bar{d}}{2T}\right)^{1/(2+\bar{d})} N^{\kappa} \tag{4}$$

with

$$\kappa = \frac{2(1+1/d_w)}{2+\bar{d}}. \tag{5}$$

Equations (1)–(5) were derived from the assumption of a free SAW. However, for the threads used in the present work, the energy depends on the threads' properties, such as elasticity (even though the modulus of elasticity may be very small, especially for the wet threads) and wetting level. The dry and wet threads should have different repulsive

J. Stat. Mech. (2019) 013401

energies for the same stretching distance. Therefore, we propose to rescale the repulsive energy for the threads as follows:

$$U \approx \phi N^2 r^{-\bar{d}} \tag{6}$$

to give the Helmholtz free energy as:

$$F \approx \phi N^2 r^{-\bar{d}} + T r^2 N^{-2/d_w} \tag{7}$$

with ϕ is a parameter that accounts for the thread properties as mentioned above. Using the same procedure as for obtaining equation (4), the distance between the thread ends is estimated as:

$$r(\phi, N) \approx \left(\frac{\phi \bar{d}}{2T}\right)^{1/(2+\bar{d})} N^{\kappa}. \tag{8}$$

If the thread is considered as N connected identical segments of the same length, a, we can write $N = L/a$, with L is the thread length. Substituting into equation (8) we get:

$$r(\phi, L) \approx \psi \phi^{1/(2+\bar{d})} L^{\kappa} \tag{9}$$

with

$$\psi \approx \frac{1}{a^{\kappa}} \left(\frac{\bar{d}}{2T}\right)^{1/(2+\bar{d})}. \tag{10}$$

Wet threads are much easier to be bend than dry ones. The parameter ψ is a material constant. Thus ϕ decreases as the wetting level increases. From equation (9) we can write:

$$\ln r(\phi, L) \approx \ln\left[\psi \phi^{1/(2+\bar{d})}\right] + \kappa \ln L. \tag{11}$$

Dekeyser *et al* [18] have shown that, for 2D SAWs, the following estimated values are acceptable: $d_w \approx 3$ and $\bar{d} \approx 2$. Substituting into equation (5) we get:

$$\kappa \approx \frac{2(1 + 1/3)}{2 + 2} = 0.666. \tag{12}$$

This value is slightly different from the theoretical estimation for a 2D SAW of 0.75. However, for a 2D SAW, $\bar{d} = 4/3$ [23, 24] and $d_w \approx 2.8$ are also acceptable. Using these values, we have another estimation for $\kappa \approx 0.8$, which is very close to the power constant belonging to 2D SAWs ($\kappa = 0.75$) and is consistent with the slopes obtained in our experimental results, i.e. between 0.794–0.895 (figure 6). Therefore, the hypothesis of a 2D SAW process for thread conformation is justifiable.

It is clear from figure 7 that d_w is almost independent of the wetting level, indicated by the slopes (κ) changing only slightly (0.834, 0.879, and 0.895) under the three conditions. By assuming $\bar{d}$ is nearly the same for all cases, κ remaining unchanged indicates that d_w is unchanged as well. Therefore the wetting level only affects the end-to-end distance.

Let us consider the effect of wetting on the energy of the thread. Based on figures 6 and 7 we clearly obtain a linear fitting of $y = ax + b$ for all data, where $y = \ln r(\phi, L)$, $x = \ln L$,

J. Stat. Mech. (2019) 013401

$a = \kappa$ and $b \approx \ln\left[\psi\phi^{1/(2+\bar{d})}\right]$. The last relationship can be rewritten as $\psi\phi^{1/(2+\bar{d})} \approx \exp(b)$. Substituting equation (10) into (11) we can write $\phi^{1/(2+\bar{d})} \propto a^{\kappa}\exp(b)$. By assuming that a^{κ} is nearly the same for the same threads under all conditions (as shown in figure 7, where κ is nearly the same for dry, alcohol wetted and water wetted wool) we can then approximate $\phi^{1/(2+\bar{d})} \propto \exp(b)$, or:

$$\phi \propto e^{(2+\bar{d})b}. \tag{13}$$

Based on the fitting results as displayed in figure 7 and using $\bar{d} \approx 2$, wetting the wool with alcohol ($b = -1.447$) reduces the energy of the thread compared to dry wool ($b = -1.338$ by 1.55), while wetting the wool with water ($b = -1.595$) reduces the energy of the thread compared to dry wool by 1.81.

In the experiment we observed that the distance between threads ends changed with time. As the falling distance increased, the end-to-end distance decreased to approximate a certain value for a very long time, implying that the end-to-end distance evolved with time. It is then challenging to explore any equations that can describe the evolution of the end-to-end distance.

The reduction of the end-to-end distance can be compared with the process of shrinkage. Thus, an equation describing the rate of shrinkage might be adopted. Weir has proposed an equation to explain the shrinkage of tendon collagen, where the length of the tendon changes as [25] $\ell = (\ell_0 - \ell_\infty)\exp(-Kt) + \ell_\infty$, with ℓ_0 is the initial length of the tendon and ℓ_∞ is the final length of the tendon (when $t \to \infty$) and K is the rate constant. We assume that the same equation applies for end-to-end distance as follows:

$$r(L,t) = (L - r(\phi,L))\exp(-Kt) + r(\phi,L) \tag{14}$$

with K in general is a function of t.

To confirm equation (14), the time required by the threads to fall over different distances was measured. Figure 8 shows a plot of end-to-end distance of wool wetted with water and multifilament wetted with water as a function of falling time. Each material was varied at three different lengths. The symbols indicate measurement results and the curves are fitting curves using equation (14). It is obvious that all data could be well fitted with equation (14), producing $R^2 > 0.87$ (mostly > 0.95).

Let us inspect figure 8(A). For $L = 0.5$ m, 0.75 m, and 1 m we have $r(\phi,0.5) = 0.12$ m, $r(\phi,0.75) = 0.17$ m, and $r(\phi,1) = 0.2$ m, respectively. If we assume that the relation $r(\phi,L) \propto L^{\kappa}$ satisfies κ aproximated to be around 0.666, then we must have $r(\phi,L_1)/r(\phi,L_2) \propto (L_1/L_2)^{0.666}$. Using $L_1 = 0.75$ m and $L_2 = 1$ m we have $r_1/r_2 = 0.85$ while $(L_1/L_2)^{0.666} = 0.83$. Then, using $L_1 = 0.5$ ans $L_2 = 1$ we have $r_1/r_2 = 0.6$ while $(L_1/L_2)^{0.666} = 0.63$. These results have a very nice consistency. Another example is figure 8(B). For $L = 0.5$ m, 0.75 m, and 1 m we have $r(\phi,0.5) = 0.21$ m, $r(\phi,0.75) = 0.254$ m, and $r(\phi,1) = 0.31$ m, respectively. Using $L_1 = 0.75$ m and $L_2 = 1$ m we have $r_1/r_2 = 0.819$ while $(L_1/L_2)^{0.666} = 0.83$. Then using $L_1 = 0.5$ and $L_2 = 1$ we have $r_1/r_2 = 0.677$ while $(L_1/L_2)^{0.666} = 0.63$. These results also have a very nice consistency.

Instead of using a constant, K, in this model the better fittings were obtained using K as a linear function of time, $K = pt + q$, where p and q are constants. Table 1 lists the parameters used to get better fitting for the data in figure 7. In all cases it was obtained

J. Stat. Mech. (2019) 013401

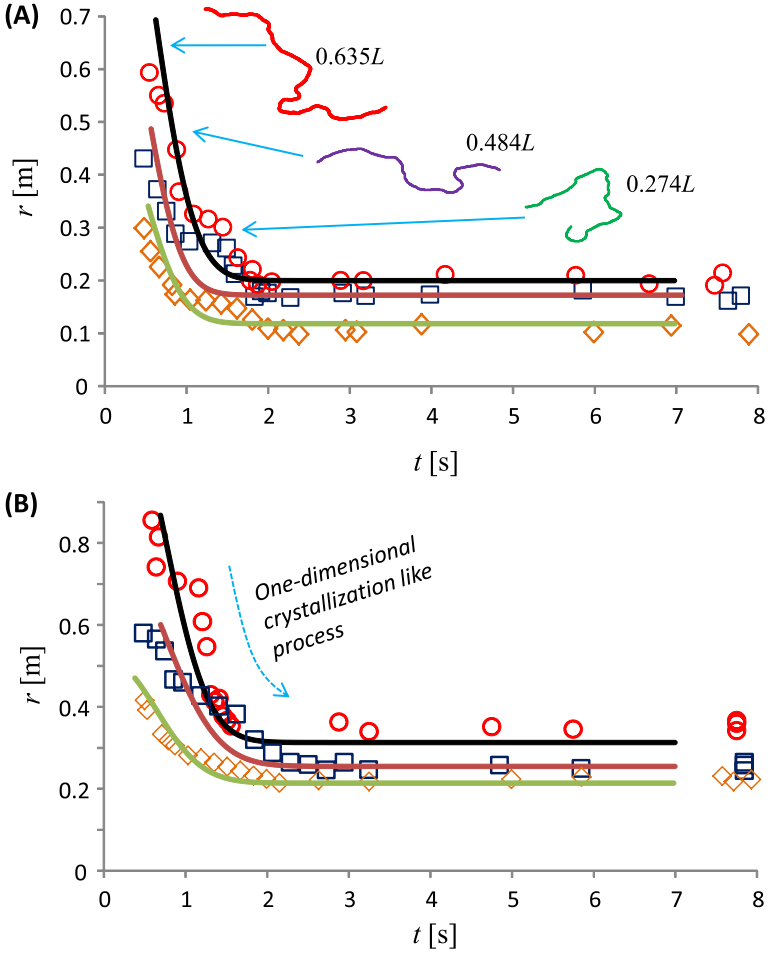

Figure 8. Plot of end-to-end distance for: (A) wool wetted with water and (B) multifilament wetted with water as a function of falling time. Each material was varied at three different lengths: (top) 1 m, (middle) 0.75 m, and (bottom) 0.5 m. The symbols indicate measurement results and the curves display the fitting curves using equation (14). The inset in figure (A) is the simulated thread conformation at different end-to-end distances.

that K increased with time. It was observed that the values of each parameter for all thread lengths were nearly identical.

Since $p > 0$ and $q < 0$ for all fitting conditions, we will identify that if $t < -q/2p$, the end-to-end distance increases with time from the moment the threads are released to fall freely. This is impossible since the maximum end-to-end distance is equal to the thread length. Therefore, we may say that the fitting equations only apply for $t > -q/2p$. Furthermore, if we inspect the value of parameters p and q we will find that $-q/2p$ is very small. For example, the largest value is $1.0706/(2 \times 1.9758) = 0.27\,\mathrm{s}$. Other values are smaller than 0.15 s.

Based on the above discussion, we can strongly state that equation (14) is able to explain the evolution of end-to-end distance of the threads with time, although some discrepancies occurred due to inaccuracies in the experiment. A possible source of inaccuracy may have been the measurement of time. The time was measured by two

J. Stat. Mech. (2019) 013401

Table 1. Parameters used for fitting the data from figure 8.

Figure	Position	p	Q
8(A)	Top	2.1980	−0.6838
	Middle	2.2888	−0.6290
	Bottom	2.5552	−0.415
8(B)	Top	1.9758	−1.0706
	Middle	1.2983	−0.3881
	Bottom	1.6011	−0.3291

people, one at an elevated position (up to 22.5 m above the ground) and one on the ground. Also, while the thread falls, the air resistance may change because of the continuous change in thread conformation until it touches the ground.

Let us further explore equation (14). Using the linear function of K resulted from fitting all data, we obtain the following equation:

$$Y = 1 - \exp\left(-p(t - t_m)^2\right) \tag{15}$$

with $t_m = -q/2p$ and Y defined as:

$$Y = 1 - \frac{r - r(\phi, L)}{L - r(\phi, L)} \exp\left(-\frac{q^2}{4p}\right). \tag{16}$$

Equation (15) is identical to the modified Avrami equation $Y = 1 - \exp\left(-p(t - t_m)^n\right)$, with t_m is known as the incubation time [26] and $n = D + 1$, with D is the dimension of space in which crystallization occurs. The Avrami equation describes the transformation of a material from one phase to another at constant temperature, where Y determines the fraction of the new phase that has been formed at time t. We are dealing with threads having 1D behaviour, $D = 1$ or $n = 2$, exactly the same as equation (16). Therefore, we can state that the process of thread conformation is likely a process of phase transformation in 1D space. The complete crystallization can be associated when the end-to-end distance is equal to $r(\phi, L)$.

Using the fitting parameters in table 1 we have $0 < q^2/4p < 0.145$ such that $0.86 < \exp(-q^2/4p) < 1$. By approximating this value with unity, we obtain the approximated form of equation (16) as:

$$Y \approx \frac{L - r}{L - r(\phi, L)}. \tag{17}$$

At very small time ($t < t_m$) we have $r \approx L$ so that $Y \approx 0$, while at $t \to \infty (r = r(\phi, L))$ we obtain $Y = 1$. Parameter t_m can be seen as adjustment time or time to start the phase transition process. Based on the data in table 1 this time ranges from 0.10 s to 0.27 s.

A simple simulation was conducted to visualize the conformation of the threads at different time lapses. The threads were divided into 1000 identical segments. The segments were placed sequentially, the direction of which was selected randomly. The first segment was placed horizontally. It was assumed that the angle made by the ith and the $(i + 1)$th segment was constant, β. After placing the first segment, the direction of the second segment was selected randomly by generating a random number, $0 \leqslant w \leqslant 1$. Suppose the angle made by the ith segment is θ_i, then the angle made by the $(i + 1)$th segment satisfies the following rule:

J. Stat. Mech. (2019) 013401

$$\theta_{i+1} = \begin{cases} \theta_i - \beta & \text{if} \quad 0 \leqslant w < 0.5 \\ \theta_i + \beta & \text{if} \quad 0.5 \leqslant w \leqslant 1 \end{cases} . \tag{18}$$

The inset in figure 8(A) shows examples of the conformation of the threads when $r = 0.635L$, $r = 0.484L$, and $r = 0.274L$. In the simulation we used $\beta = 7°$. It can clearly be seen that the conformations produced by the simulation almost perfectly match the images in figures 1 and 2.

As a final note we state here that the simple phenomenon of a free-falling thread is able to replicate two famous physical phenomena: a 2D random walk and crystallization in 1D space as described by the modified Avrami equation. The two latter phenomena occur at microscopic scale. Therefore, the present experiment was able to manisfest or replicate two microscopic processes at macroscopic scale that can be easily observed with the naked eye.

5. Conclusion

Conducting an experiment on free-falling threads and modelling their behavior based on the experimental results was successful in bringing two microscopic processes (a 2D SAW and phase transition in 1D space according to the modified Avrami equation) to macroscopic scale, a process that can easily be observed with the naked eye. The dependence of the thread's end-to-end distance on the thread length satisfies a scaling relation that is exactly the same as the scaling relation in a 2D SAW. The equation describing the evolution of the thread's end-to-end distance with time is precisely the same as the evolution of the crystallization process described by the modified Avrami equation. This is very surprising since a simple phenomenon from daily life indeed was proven to contain very rich physical ingredients.

Acknowledgment

The PMDSU (Program Magister Doktor Sarjana Unggul) research grant from the Ministry of Research and Higher Education, Republic of Indonesia No. 535C/I1.C01/PL/2018 for HDR is gratefully acknowledged.

References

[1] Zimmt M B, Peterson K A and Fayer M D 1988 Short polymer chain statistics and the relationship to end to end electronic excitation transport: random walks with variable step lengths *Macromolecules* **21** 1145–54
[2] Gentien P, Lunven M, Lazure P and Youenou A 2007 Motility and autotoxicity in Karenia mikimotoi (Dinophyceae) *Phil. Trans. R. Soc.* B **362** 1487
[3] Flory P J and Volkenstein M 1969 Statistical mechanics of chain molecules *Biopolymers* **8** 699–700
[4] Mazur J 1965 Distribution function of the end-to-end distances of linear polymers with excluded volume effects *J. Res. Natl Bur. Stand.* **69A** 355
[5] Miller J T, Lazarus A, Audoly B and Reis P M 2014 Shapes of a suspended curly hair *Phys. Rev. Lett.* **112** 068103

J. Stat. Mech. (2019) 013401

[6] Bertails F, Audoly B, Cani M-P, Querleux B, Leroy F and Lévêque J-L 2006 Super-helices for predicting the dynamics of natural hair *ACM Trans. Graph.* **25** 1180
[7] Rahmayanti H D, Utami F D and Abdullah M 2016 Physics model for wringing of wet cloth *Eur. J. Phys.* **37** 065806
[8] Karamouzas I, Skinner B and Guy S J 2014 Universal power law governing pedestrian interactions *Phys. Rev. Lett.* **113** 238701
[9] Mayer H C and Krechetnikov R 2012 Walking with coffee: why does it spill? *Phys. Rev.* E **85** 046117
[10] Abdullah M, Khairunnisa S and Akbar F 2014 Bending of sparklers *Eur. J. Phys.* **35** 035019
[11] Buchak P, Eloy C and Reis P M 2010 The clapping book: wind-driven oscillations in a stack of elastic sheets *Phys. Rev. Lett.* **105** 194301
[12] Wibowo E, Rokhmat M, Sutisna S, Yuliza E, Khairurrijal K and Abdullah M 2016 The dynamics of a cylinder containing granules rolling down an inclined plane *Powder Technol.* **301** 44–57
[13] Weon B M and Je J H 2010 Capillary force repels coffee-ring effect *Phys. Rev.* E **82** 015305
[14] Weon B M and Je J H 2013 Fingering inside the coffee ring *Phys. Rev.* E **87** 013003
[15] Bonnel W S, Byman L and Keyes D B 1940 Surface tension of ethyl alcohol–water mixtures *Ind. Eng. Chem.* **32** 532–34
[16] Adamson A W and Gast A P 1967 *Physical Chemistry of Surfaces* (New York: Wiley)
[17] De Gennes P G and Gennes P G 1979 *Scaling Concepts in Polymer Physics* (London: Cornell University Press)
[18] Dekeyser R, Maritan A and Stella A 1987 Random walks with intersections: static and dynamic fractal properties *Phys. Rev.* A **36** 2338–51
[19] Isaacson J and Lubensky T C 1980 Flory exponents for generalized polymer problems *J. Physique Lett.* **41** 469–71
[20] Rosato A, Strandburg K J, Prinz F and Swendsen R H 1987 Why the Brazil nuts are on top: size segregation of particulate matter by shaking *Phys. Rev. Lett.* **58** 1038
[21] Barrat A, Trizac E and Ernst M H 2005 Granular gases: dynamics and collective effects *J. Phys.: Condens. Matter* **17** S2429
[22] Bobylev A V, Cercignani C and Gamba I M 2009 Generalized kinetic Maxwell type models of granular gases (arXiv:0901.3864v1)
[23] Alexander S and Orbach R 1982 Density of states on fractals: 'fractons' *J. Physique Lett.* **43** 625–31
[24] Rammal R and Toulouse G 1983 Random walks on fractal structures and percolation clusters *J. Phys. Lett.* **44** 13–22
[25] Weir B C E 1949 Rate of shrinkage of tendon collagen: heat, entropy, and free energy of activation of the shrinkage of untreated tendon; effect of acid, salt, pickle, and tannage on the activation of tendon collagen *J. Res. Natl Bur. Stand.* **42** 17–32
[26] Sinha I and Mandal R K 2011 Avrami exponent under transient and heterogeneous nucleation transformation conditions *J. Non-Cryst. Solids* **357** 919–25

J. Stat. Mech. (2019) 013401